Analysis of variable coefficient advection–diffusion problems via complex variable reproducing kernel particle method*

Weng Yun-Jie(翁云杰)[a)b)] and Cheng Yu-Min(程玉民)[a)†]

[a)] *Shanghai Institute of Applied Mathematics and Mechanics, Shanghai Key Laboratory of Mechanics in Energy Engineering, Shanghai University, Shanghai* 200072, *China*

[b)] *Ningbo Institute of Technology, Zhejiang University, Ningbo* 315100, *China*

(Received 16 December 2012; revised manuscript received 26 February 2013)

The complex variable reproducing kernel particle method (CVRKPM) of solving two-dimensional variable coefficient advection–diffusion problems is presented in this paper. The advantage of the CVRKPM is that the shape function of a two-dimensional problem is formed with a one-dimensional basis function. The Galerkin weak form is employed to obtain the discretized system equation, and the penalty method is used to apply the essential boundary conditions. Then the corresponding formulae of the CVRKPM for two-dimensional variable coefficient advection–diffusion problems are obtained. Two numerical examples are given to show that the method in this paper has greater accuracy and computational efficiency than the conventional meshless method such as reproducing the kernel particle method (RKPM) and the element-free Galerkin (EFG) method.

Keywords: meshless method, reproducing kernel particle method (RKPM), complex variable reproducing kernel particle method (CVRKPM), advection–diffusion problem

PACS: 02.60.Cb, 02.60.Lj, 66.10.C−, 82.56.Lz **DOI:** 10.1088/1674-1056/22/9/090204

1. Introduction

The advection–diffusion equations are important in many fields in engineering.[1–5] In general, the advection–diffusion equations are solved using numerical methods, such as the finite difference method (FDM), the finite element method (FEM), and the boundary element method (BEM). These methods are derived from local interpolation schemes and require a mesh to support the application.[6]

Meshless methods are approximate methods that are based on nodes without initial mesh and re-meshing.[7–10] Then, the meshless method can overcome the disadvantage that the conventional numerical method depends on the mesh of the solution domain. At present, the element-free Galerkin (EFG) method[11–17] and the reproducing kernel particle method (RKPM)[18–20] are the most important meshless methods. To overcome the disadvantage that the EFG method and the RKPM have a great computational cost, based on the complex variable theory, the complex variable meshless methods, such as the complex variable element-free Galerkin (CVEFG) method[21–30] and the complex variable reproducing kernel particle method (CVRKPM)[31,32] have been presented. The advantage of a complex variable meshless method is that the correction function of a two-dimensional (2D) problem is formed with a one-dimensional (1D) basis function when the shape function is obtained, which leads to fewer nodes selected in the domain of the problem without the loss of the computational accuracy.[33] Then, the complex variable meshless method has a higher computational accuracy and efficiency.[34]

In this paper, the CVRKPM of solving 2D variable coefficient advection–diffusion problems is proposed. The Galerkin weak form is employed to obtain the discretized system equation, and the penalty method is used to apply the essential boundary conditions. Then, the corresponding formulae of the CVRKPM for 2D variable coefficient advection–diffusion problems are obtained. Two numerical examples are given to show that the method in this paper has greater accuracy and computational efficiency than the conventional meshless method, such as the RKPM and EFG methods.

2. Shape function of the CVRKPM

Consider a complex function $\bar{u}(z)$ which is the continuous derivative function defined in the domain Ω. In the CVRKPM, the approximate function $\bar{u}^{\mathrm{h}}(z)$ at point z is

$$\begin{aligned}\bar{u}^{\mathrm{h}}(z) &= \bar{u}_1^{\mathrm{h}}(z)+\mathrm{i}\bar{u}_2^{\mathrm{h}}(z)\\ &= \int_{\Omega}^{\bar{u}(z')} \bar{w}_{\mathrm{h}}(z-z')\,\mathrm{d}z', \quad (z=x_1+\mathrm{i}x_2\in\Omega),\end{aligned} \tag{1}$$

where $\bar{w}_{\mathrm{h}}(z-z')$ is a corrected reproducing kernel function expressed as

$$\bar{w}_{\mathrm{h}}(z-z') = C(z;z-z')w_{\mathrm{h}}(z-z'). \tag{2}$$

Here, $w_{\mathrm{h}}(z-z')$ is the kernel function which has a compact support domain, and $C(z;z-z')$ is the correction function which is expressed as a linear combination of polynomial basis

*Project supported by the National Natural Science Foundation of China (Grant No. 11171208) and the Leading Academic Discipline Project of Shanghai City, China (Grant No. S30106).

†Corresponding author. E-mail: ymcheng@shu.edu.cn

© 2013 Chinese Physical Society and IOP Publishing Ltd

functions, i.e.,

$$C(z;z-z') = \sum_{i=0}^{m} p_i(z-z')b_i(z) = \boldsymbol{p}^{\mathrm{T}}(z-z')\boldsymbol{b}(z), \quad (z\in\Omega). \tag{3}$$

The discretized form of the complex variables reproducing kernel approximation can be obtained by applying the trapezoidal rule to Eq. (1), i.e.,

$$\bar{u}^{\mathrm{h}}(z) = \sum_{I=1}^{n} C(z;z-z_I)w_{\mathrm{h}}(z-z_I)\Delta V_I\bar{u}(z_I), \tag{4}$$

where z_I is the node in the support domain of z, n is the total number of the nodes in the support domain of z,

$$\bar{u}(z_I) = \bar{u}_1(z_I) + \mathrm{i}\bar{u}_2(z_I), \tag{5}$$

and ΔV_I is the volume of node z_I and represents the integration weight, i.e.,

$$\sum_{I=1}^{n_{\mathrm{t}}} \Delta V_I = \Omega, \tag{6}$$

where n_{t} is the total number of nodes distributed in the solution domain.

Equation (4) can be rewritten as

$$\bar{u}^{\mathrm{h}}(z) = \boldsymbol{C}(z)\boldsymbol{W}(z)\boldsymbol{V}\cdot\bar{u}, \tag{7}$$

where

$$\bar{\boldsymbol{u}} = (\bar{u}(z_1),\bar{u}(z_2),\ldots,\bar{u}(z_n))^{\mathrm{T}} = \boldsymbol{Q}\boldsymbol{u}, \tag{8}$$

$$\boldsymbol{u} = (u_1(z_1),u_2(z_1),u_1(z_2),u_2(z_2),\ldots,u_1(z_n),u_2(z_n))^{\mathrm{T}}, \tag{9}$$

$$\boldsymbol{Q} = \begin{bmatrix} 1 & \mathrm{i} & 0 & 0 & 0 & 0 & \cdots & 0 & 0 \\ 0 & 0 & 1 & \mathrm{i} & 0 & 0 & \cdots & 0 & 0 \\ 0 & 0 & 0 & 0 & 1 & \mathrm{i} & \cdots & 0 & 0 \\ \vdots & \vdots & \vdots & \vdots & \vdots & \vdots & \ddots & \vdots & \vdots \\ 0 & 0 & 0 & 0 & 0 & 0 & \cdots & 1 & \mathrm{i} \end{bmatrix}_{n\times 2n}, \tag{10}$$

$$\boldsymbol{W}(z) = \begin{bmatrix} w(z-z_1) & 0 & \cdots & 0 \\ 0 & w(z-z_2) & \cdots & 0 \\ \vdots & \vdots & \ddots & \vdots \\ 0 & 0 & \cdots & w(z-z_n) \end{bmatrix}, \tag{11}$$

$$\boldsymbol{V} = \begin{bmatrix} \Delta V_1 & 0 & \cdots & 0 \\ 0 & \Delta V_2 & \cdots & 0 \\ \vdots & \vdots & \ddots & \vdots \\ 0 & 0 & \cdots & \Delta V_n \end{bmatrix}. \tag{12}$$

Let

$$C_I(z) = C_I(z;z-z_I) = \boldsymbol{p}^{\mathrm{T}}(z-z_I)\boldsymbol{b}(z), \tag{13}$$

then we have

$$\boldsymbol{C}(z) = (C_1(z),C_2(z),\ldots,C_n(z)) = \boldsymbol{b}^{\mathrm{T}}(z)\boldsymbol{P}, \tag{14}$$

where

$$\boldsymbol{P} = \begin{bmatrix} p_0(z-z_1) & p_0(z-z_2) & \cdots & p_0(z-z_n) \\ p_1(z-z_1) & p_1(z-z_2) & \cdots & p_1(z-z_n) \\ \vdots & \vdots & \ddots & \vdots \\ p_m(z-z_1) & p_m(z-z_2) & \cdots & p_m(z-z_n) \end{bmatrix}. \tag{15}$$

Here, the correction coefficients are obtained via the reproducing conditions of the trial function, and

$$\boldsymbol{M}(z)\cdot\boldsymbol{b}(z) = \boldsymbol{H}, \tag{16}$$

where

$$\boldsymbol{M}(z) = \sum_{I=1}^{n} \boldsymbol{p}(z-z_I)\cdot\boldsymbol{p}^{\mathrm{T}}(z-z_I)\cdot w_{\mathrm{h}}(z-z_I)\cdot\Delta V_I, \tag{17}$$

$$\boldsymbol{H} = (1,0,\ldots,0)^{\mathrm{T}}, \tag{18}$$

$$\boldsymbol{b}(z) = \boldsymbol{M}^{-1}(z)\cdot\boldsymbol{H}. \tag{19}$$

Then, the expression of the trial function $\bar{u}^{\mathrm{h}}(z)$ can be written as

$$\bar{u}^{\mathrm{h}}(z) = \boldsymbol{\Phi}(z)\bar{\boldsymbol{u}} = \sum_{I=1}^{n} \Phi_I(z)\bar{u}(z_I), \tag{20}$$

where $\boldsymbol{\Phi}(z)$ is defined as the shape function of the CVRKPM,

$$\boldsymbol{\Phi}(z) = (\Phi_1(z),\Phi_2(z),\ldots,\Phi_n(z)) = \boldsymbol{C}(z)\cdot\boldsymbol{W}(z)\cdot\boldsymbol{V}. \tag{21}$$

Then,

$$u_1^{\mathrm{h}}(z) = \mathrm{Re}[\boldsymbol{\Phi}(z)\bar{\boldsymbol{u}}] = \mathrm{Re}[\sum_{I=1}^{n} \Phi_I(z)\bar{u}(z_I)], \tag{22}$$

$$u_2^{\mathrm{h}}(z) = \mathrm{Im}[\boldsymbol{\Phi}(z)\bar{\boldsymbol{u}}] = \mathrm{Im}[\sum_{I=1}^{n} \Phi_I(z)\bar{u}(z_I)]. \tag{23}$$

The advantage of the CVRKPM is that the shape function of a 2D problem is formed with a 1D basis function, which leads to the fact that fewer nodes can be selected in the meshless method formed with the CVRKPM under the same accuracy. As for an arbitrary node, when its shape function and its derivatives are calculated, it is necessary to obtain the inversion of the matrix $\boldsymbol{M}$. Under the same accuracy, because of fewer unknown coefficients needed in the CVRKPM approximation, which leads to the reduction of the dimension of the matrix, then the CVRKPM has a great computational efficiency compared with the RKPM.[16]

3. CVRKPM for 2D advection–diffusion problems

Now we consider the time-dependent variable coefficient advection–diffusion equation

$$\frac{\partial u}{\partial t} - d_1(x_1,x_2)\frac{\partial^2 u}{\partial x_1^2} - d_2(x_1,x_2)\frac{\partial^2 u}{\partial x_2^2} + v_1(x_1,x_2)\frac{\partial u}{\partial x_1} + v_2(x_1,x_2)\frac{\partial u}{\partial x_2} = f(x_1,x_2,t), \quad (x_1,x_2)\in\Omega,\ t\geq 0, \tag{24}$$

with the boundary conditions below,

$$u(x_1,x_2,t) = \bar{u}(x_1,x_2,t), \quad (x_1,x_2)\in\Gamma^u, \tag{25}$$

$$d_1(x_1,x_2)\frac{\partial u(x_1,x_2,t)}{\partial x_1}n_1+d_2(x_1,x_2)\frac{\partial u(x_1,x_2,t)}{\partial x_2}n_2 = \bar{q}(x_1,x_2,t), \quad (x_1,x_2)\in\Gamma^q, \tag{26}$$

and the initial condition of

$$u(x_1,x_2,0)=u_0, \tag{27}$$

where $u(x_1,x_2,t)$ is a field function at the point $x=(x_1,x_2)$ and time t; $d_i(x_1,x_2)$ is the diffusion coefficient; $v_i(x_1,x_2)$ is the advection coefficients in the x_i direction; $f(x_1,x_2,t)$ is the source term; $\bar{u}(x_1,x_2,t)$ and $\bar{q}(x_1,x_2,t)$ are the prescribed functions on the corresponding boundaries Γ^u and Γ^q, respectively; n_i is the outward unit normal to the boundary Γ in the x_i direction; $\Gamma^u\cup\Gamma^q=\Gamma$; $\Gamma^u\cap\Gamma^q=\emptyset$.

Using the penalty method to enforce the essential boundary conditions, the corresponding constrained Galerkin weak form of the time-dependent advection–diffusion problem can be obtained as

$$\begin{aligned}&\int_\Omega \delta u\Big(\frac{\partial u}{\partial t}-f\Big)\mathrm{d}\Omega+\int_\Omega \delta(\boldsymbol{L}u)^{\mathrm{T}}\tilde{\boldsymbol{d}}(\boldsymbol{L}u)\mathrm{d}\Omega\\&+\int_\Omega \delta u\Big(v_1(x_1,x_2)\frac{\partial u}{\partial x_1}+v_2(x_1,x_2)\frac{\partial u}{\partial x_2}\Big)\mathrm{d}\Omega\\&-\int_{\Gamma^q}\delta u\bar{q}\mathrm{d}\Gamma+\int_{\Gamma^u}\delta(u-\bar{u})\alpha(u-\bar{u})\mathrm{d}\Gamma,\end{aligned} \tag{28}$$

where α is the penalty factor,

$$\tilde{\boldsymbol{d}}=\begin{bmatrix}d_1(x_1,x_2) & 0\\ 0 & d_2(x_1,x_2)\end{bmatrix}, \tag{29}$$

$$\boldsymbol{L}(\cdot)=\begin{bmatrix}\dfrac{\partial}{\partial x_1}\\ \dfrac{\partial}{\partial x_2}\end{bmatrix}(\cdot). \tag{30}$$

From Eq. (28), we have

$$\begin{aligned}&\int_\Omega \delta u\frac{\partial u}{\partial t}\mathrm{d}\Omega-\int_\Omega \delta uf\mathrm{d}\Omega+\int_\Omega\delta(\boldsymbol{L}u)^{\mathrm{T}}\tilde{\boldsymbol{d}}(\boldsymbol{L}u)\mathrm{d}\Omega\\&+\int_\Omega \delta uv_1(x_1,x_2)\frac{\partial u}{\partial x_1}\mathrm{d}\Omega+\int_\Omega\delta uv_2(x_1,x_2)\frac{\partial u}{\partial x_2}\mathrm{d}\Omega\\&-\int_{\Gamma^q}\delta u\bar{q}\mathrm{d}\Gamma+\int_{\Gamma^u}\delta u\alpha u\mathrm{d}\Gamma-\int_{\Gamma^u}\delta u\alpha\bar{u}\mathrm{d}\Gamma.\end{aligned} \tag{31}$$

From Eq. (22), we can obtain the following approximations:

$$\begin{aligned}\boldsymbol{u}(\boldsymbol{z},\boldsymbol{t})&=\mathrm{Re}[\boldsymbol{\Phi}(\boldsymbol{z})u(\boldsymbol{t})]=\sum_{\boldsymbol{I}=1}^{\boldsymbol{n}}\mathrm{Re}[\boldsymbol{\Phi}_{\boldsymbol{I}}(\boldsymbol{z})]\boldsymbol{u}_{\boldsymbol{I}}(\boldsymbol{t})\\&=\sum_{\boldsymbol{I}=1}^{\boldsymbol{n}}\tilde{\boldsymbol{\Phi}}_{\boldsymbol{I}}(\boldsymbol{z})\boldsymbol{u}_{\boldsymbol{I}}(\boldsymbol{t})=\tilde{\boldsymbol{\Phi}}(\boldsymbol{z})u,\end{aligned} \tag{32}$$

$$\begin{aligned}\frac{\partial\boldsymbol{u}(\boldsymbol{z},\boldsymbol{t})}{\partial\boldsymbol{t}}&=\frac{\partial}{\partial t}\sum_{\boldsymbol{I}=1}^{\boldsymbol{n}}\tilde{\boldsymbol{\Phi}}_{\boldsymbol{I}}(\boldsymbol{z})\boldsymbol{u}_{\boldsymbol{I}}(\boldsymbol{t})\\&=\sum_{\boldsymbol{I}=1}^{\boldsymbol{n}}\tilde{\boldsymbol{\Phi}}_{\boldsymbol{I}}(\boldsymbol{z})\frac{\partial\boldsymbol{u}_{\boldsymbol{I}}(\boldsymbol{t})}{\partial t}=\tilde{\boldsymbol{\Phi}}(\boldsymbol{z})\dot{\boldsymbol{u}},\end{aligned} \tag{33}$$

where n is the node number in the compact support domain of z, and

$$\tilde{\boldsymbol{\Phi}}(z)=(\tilde{\boldsymbol{\Phi}}_1(z),\tilde{\boldsymbol{\Phi}}_2(z),\cdots,\tilde{\boldsymbol{\Phi}}_n(z)), \tag{34}$$

$$\boldsymbol{u}=(\boldsymbol{u}_1(t),\boldsymbol{u}_2(t),\ldots,\boldsymbol{u}_{\boldsymbol{n}}(t))^{\mathrm{T}}, \tag{35}$$

$$\begin{aligned}\boldsymbol{L}u(\boldsymbol{z},t)&=\sum_{\boldsymbol{I}=1}^{\boldsymbol{n}}\begin{bmatrix}\dfrac{\partial}{\partial\boldsymbol{x}_1}\\ \dfrac{\partial}{\partial\boldsymbol{x}_2}\end{bmatrix}\mathrm{Re}[\boldsymbol{\Phi}_{\boldsymbol{I}}(\boldsymbol{z})]\boldsymbol{u}_{\boldsymbol{I}}(\boldsymbol{t})\\&=\sum_{\boldsymbol{I}=1}^{\boldsymbol{n}}\boldsymbol{B}_{\boldsymbol{I}}(\boldsymbol{z})\cdot\boldsymbol{u}_{\boldsymbol{I}}(\boldsymbol{t})=\boldsymbol{B}(\boldsymbol{z})\cdot\boldsymbol{u}.\end{aligned} \tag{36}$$

Substituting Eqs. (34)–(36) into Eq. (32) yields

$$\begin{aligned}&\int_\Omega\delta[\tilde{\boldsymbol{\Phi}}(\boldsymbol{z})u][\tilde{\boldsymbol{\Phi}}(\boldsymbol{z})\dot{u}]\mathrm{d}\Omega-\int_\Omega\delta[\tilde{\boldsymbol{\Phi}}(\boldsymbol{z})u]\boldsymbol{f}\mathrm{d}\Omega\\&+\int_\Omega\delta[B(\boldsymbol{z})u]^{\mathrm{T}}\tilde{d}[B(\boldsymbol{z})u]\mathrm{d}\Omega\\&+\int_\Omega\delta[\tilde{\boldsymbol{\Phi}}(z)\boldsymbol{u}]v_1(x_1,x_2)\frac{\partial}{\partial x_1}\tilde{\boldsymbol{\Phi}}(z)\boldsymbol{u}\mathrm{d}\Omega\\&+\int_\Omega\delta[\tilde{\boldsymbol{\Phi}}(z)\boldsymbol{u}]v_2(x_1,x_2)\frac{\partial}{\partial x_2}\tilde{\boldsymbol{\Phi}}(z)\boldsymbol{u}\mathrm{d}\Omega\\&-\int_{\Gamma^q}\delta[\tilde{\boldsymbol{\Phi}}(z)\boldsymbol{u}]\bar{q}\mathrm{d}\Gamma+\int_{\Gamma^u}\delta[\tilde{\boldsymbol{\Phi}}(z)\boldsymbol{u}]\alpha[\tilde{\boldsymbol{\Phi}}(z)\boldsymbol{u}]\mathrm{d}\Gamma\\&-\int_{\Gamma^u}\delta[\tilde{\boldsymbol{\Phi}}(z)\boldsymbol{u}]\alpha\bar{u}\mathrm{d}\Gamma=0.\end{aligned} \tag{37}$$

Equation (35) can be written as

$$\begin{aligned}&\delta\boldsymbol{u}^{\mathrm{T}}(\boldsymbol{C}\dot{u}+\boldsymbol{D}u+\boldsymbol{K}^{\alpha}\boldsymbol{u}+\boldsymbol{G}^{(1)}\boldsymbol{u}+\boldsymbol{G}^{(2)}\boldsymbol{u}-\boldsymbol{F}^{(1)}\\&-\boldsymbol{F}^{(2)}-\boldsymbol{F}^{\alpha})=0,\end{aligned} \tag{38}$$

where

$$\boldsymbol{C}=\int_\Omega\tilde{\boldsymbol{\Phi}}^{\mathrm{T}}(\boldsymbol{z})\tilde{\boldsymbol{\Phi}}(\boldsymbol{z})\mathrm{d}\Omega, \tag{39}$$

$$\boldsymbol{D}=\int_\Omega B^{\mathrm{T}}(\boldsymbol{z})\tilde{d}B(\boldsymbol{z})\mathrm{d}\Omega, \tag{40}$$

$$\boldsymbol{K}^{\boldsymbol{\alpha}}=\int_{\Gamma^u}\tilde{\boldsymbol{\Phi}}^{\mathrm{T}}(\boldsymbol{z})\boldsymbol{\alpha}\tilde{\boldsymbol{\Phi}}(\boldsymbol{z})\mathrm{d}\Gamma, \tag{41}$$

$$\boldsymbol{G}^{(1)}=\int_\Omega\tilde{\boldsymbol{\Phi}}^{\mathrm{T}}(\boldsymbol{z})v_1(x_1,x_2)\frac{\partial}{\partial x_1}\tilde{\boldsymbol{\Phi}}(\boldsymbol{z})\mathrm{d}\Omega, \tag{42}$$

$$\boldsymbol{G}^{(2)}=\int_\Omega\tilde{\boldsymbol{\Phi}}^{\mathrm{T}}(\boldsymbol{z})v_2(x_1,x_2)\frac{\partial}{\partial x_2}\tilde{\boldsymbol{\Phi}}(\boldsymbol{z})\mathrm{d}\Omega, \tag{43}$$

$$\boldsymbol{F}^{(1)}=\int_\Omega\tilde{\boldsymbol{\Phi}}^{\mathrm{T}}(z)\boldsymbol{f}\mathrm{d}\Omega, \tag{44}$$

$$\boldsymbol{F}^{(2)}=\int_{\Gamma^q}\tilde{\boldsymbol{\Phi}}^{\mathrm{T}}\bar{q}\mathrm{d}\Gamma, \tag{45}$$

$$\boldsymbol{F}^{\boldsymbol{\alpha}}=\int_{\Gamma^u}\tilde{\boldsymbol{\Phi}}^{\mathrm{T}}(\boldsymbol{z})\boldsymbol{\alpha}\bar{\boldsymbol{u}}\mathrm{d}\Gamma. \tag{46}$$

In the advection–diffusion problem, the field function u is not only a function of space coordinates, but also depends on time. Because the time and space domain are not coupled, we apply the CVRKPM in the space domain, and the finite difference method in the time domain. We can obtain the final linear system as

$$\boldsymbol{C}\dot{\boldsymbol{u}}+\bar{\boldsymbol{K}}\boldsymbol{u}=\bar{\boldsymbol{F}}, \tag{47}$$

where

$$\bar{\boldsymbol{K}}=\boldsymbol{D}+\boldsymbol{K}^{\alpha}+\boldsymbol{G}^{(1)}+\boldsymbol{G}^{(2)}, \tag{48}$$

$$\bar{\boldsymbol{F}}=\boldsymbol{F}^{(1)}+\boldsymbol{F}^{(2)}+\boldsymbol{F}^{\alpha}. \tag{49}$$

Equation (47) is a system of linear ordinary differential equations, in which the time is an independent variable. Sup-

pose that the time step is Δt. Using the traditional difference method for two-point boundary value problems, we can establish the relationship between $u|_{t+\Delta t}$ and $u|_t$ as

$$\theta \frac{\partial u}{\partial t}\Big|_{t+\Delta t} + (1-\theta)\frac{\partial u}{\partial t}\Big|_{t} = \frac{u|_{t+\Delta t} - u|_t}{\Delta t}. \tag{50}$$

From Eq. (47), we can obtain $\frac{\partial u}{\partial t}|_{t+\Delta t}$ and $\frac{\partial u}{\partial t}|_t$. Then, substituting the results into Eq. (50) yields

$$\Big(\frac{C}{\Delta t} + \theta \bar{K}|_{t+\Delta t}\Big)\boldsymbol{u}|_{t+\Delta t} = \Big(\frac{C}{\Delta t} - (1-\theta)\bar{K}|_t\Big)\boldsymbol{u}|_t + \theta \bar{F}|_{t+\Delta t} + (1-\theta)\bar{F}|_t, \tag{51}$$

where θ is a time-weighed coefficient, and its different values correspond to different time difference forms. When $\theta = 1/2$, equation (51) becomes

$$\Big(\frac{2C}{\Delta t} + \bar{K}|_{t+\Delta t}\Big)\boldsymbol{u}|_{t+\Delta t} = \Big(\frac{2C}{\Delta t} - \bar{K}|_t\Big)\boldsymbol{u}|_t + \bar{F}|_{t+\Delta t} + \bar{F}|_t. \tag{52}$$

Then, the relationship between $\boldsymbol{u}|_{t+\Delta t}$ and $\boldsymbol{u}|_t$ is obtained. With the initial condition, starting from the initial time, we solve the field function at the next moment after a time step. The field function $\boldsymbol{u}$ at any time can be achieved step by step.

4. Numerical examples

For the validation of the method described above, we present two examples. In the examples, we examine the accuracy of CVRKPM and make comparisons between the CVRKPM, RKPM, and EFG methods.

4.1. Advection-dominated equation

Consider the following linear advection–diffusion equation:

$$\frac{\partial u}{\partial t} + \frac{\partial u}{\partial x_1} + \frac{\partial u}{\partial x_2} - \frac{1}{4\pi^2}\Big(\frac{\partial^2 u}{\partial x_1^2} + \frac{\partial^2 u}{\partial x_2^2}\Big) = \pi \mathrm{e}^{-t}(\pi(x_1 + x_2)),$$
$$(x_1, x_2) \in \Omega = [0,1] \times [0,1], \quad t \geq 0, \tag{53}$$

together with Dirichlet-type boundary conditions

$$u(0, x_2, t) = 0, \tag{54}$$
$$u(1, x_2, t) = 0, \tag{55}$$
$$u(x_1, 0, t) = 0, \tag{56}$$
$$u(x_1, 1, t) = 0, \tag{57}$$

and the initial condition

$$u(x_1, x_2, 0) = \sin(\pi x_1)\sin(\pi x_2), \quad (x_1, x_2) \in \Omega. \tag{58}$$

The analytical solution is given by

$$u(x_1, x_2, t) = \mathrm{e}^{-t}\sin(\pi x_1)\sin(\pi x_2). \tag{59}$$

This is an advection-dominated advection–diffusion equation. To illustrate the accuracy of the proposed meshless method, we choose 12×12 regularly distributed nodes. The following parameters are employed to solve Eq. (53): $\alpha = 1.0 \times 10^3$ and $\Delta t = 0.001$. The $d_{\max}$ is chosen to reach the highest accuracy of each method. In experiment, we assign $d_{\max} = 1.7$ for CVRKPM, $d_{\max} = 2.5$ for RKPM, and $d_{\max} = 1.9$ for the EFG method.

Figures 1–3 show the analytical and numerical solutions obtained, respectively, by the CVRKPM, the EFG method, and the RKPM when $x_1 = 1/12$ at $t = 0.1$, 0.2, and 0.5 s. We can see that the results of the three methods are in very good agreement with the exact solutions. It is obvious that the CVRKPM has a higher accuracy than the EFG method and the RKPM.

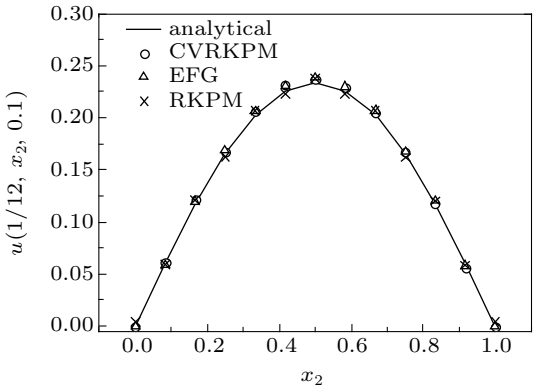


Fig. 1. Comparison of the solutions of CVRKPM, RKPM, and EFG method with the analytical one at $x_1 = 1/12$ at time $t = 0.1$ s.

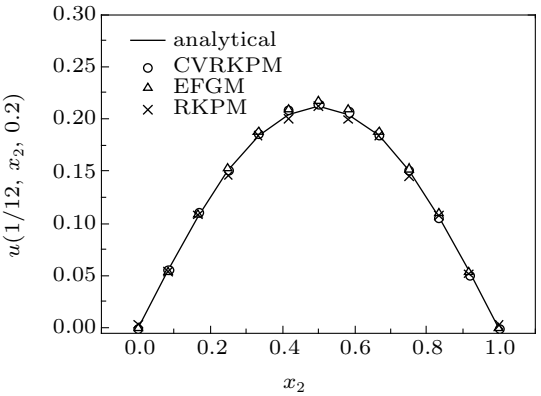


Fig. 2. Comparison of the solutions of CVRKPM, RKPM, and EFG method with the analytical one at $x_1 = 1/12$ at time $t = 0.2$ s.

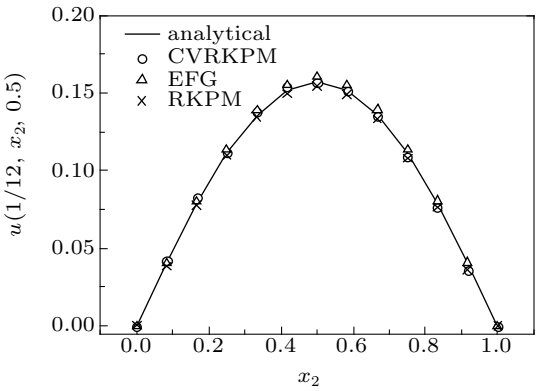


Fig. 3. Comparison of the solutions of CVRKPM, RKPM, and EFG method with the analytical one at $x_1 = 1/12$ at time $t = 0.5$ s.

As regards the computational speeds of the three methods, under the same accuracy, the CVRKPM is faster than the

other two methods. As shown in Fig. 4, under the same accuracy, the CVRKPM requires 144 nodes and CPU time of 47 s, the EFG mothod requires 169 nodes and CPU time of 85 s, and the RKPM requires 196 nodes and CPU time of 93 s. Thus, the CVRKPM has higher computational efficiency.

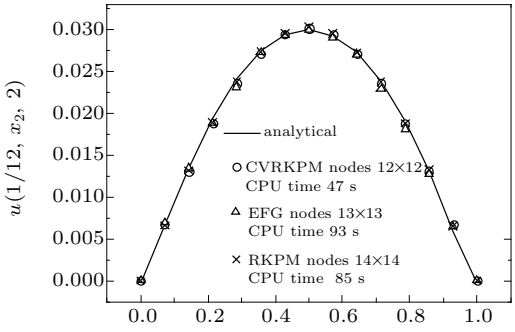


Fig. 4. Comparison of CPU time for a given accuracy at $x_1 = 1/12$ at time $t = 2$ s.

4.2. Diffusion-dominated equation

Consider the following advection–diffusion equation:

$$\frac{\partial u}{\partial t} + \frac{1}{2}x_1\frac{\partial u}{\partial x_1} + \frac{1}{2}x_2\frac{\partial u}{\partial x_2} - \left(\frac{\partial^2 u}{\partial x_1^2} + \frac{\partial^2 u}{\partial x_2^2}\right) = 0,$$
$$(x_1, x_2) \in \Omega = [0,1]\times[0,1],\ t \geq 0, \qquad (60)$$

together with the Dirichlet-type boundary conditions

$$u(0, x_2, t) = 0, \qquad (61)$$
$$u(1, x_2, t) = x_2\,\mathrm{e}^{-t}, \qquad (62)$$
$$u(x_1, 0, t) = 0, \qquad (63)$$
$$u(x_1, 1, t) = x_1\,\mathrm{e}^{-t}, \qquad (64)$$

and the initial condition

$$u(x_1, x_2, 0) = x_1 x_2, \quad (x_1, x_2) \in \Omega. \qquad (65)$$

The analytical solution is given by

$$u(x_1, x_2, t) = x_1 x_2\,\mathrm{e}^{-t}. \qquad (66)$$

This is a diffusion-dominated advection–diffusion equation. This example is solved using the CVRKPM, the EFG method, and the RKPM with totally 144 regularly distributed nodes. The penalty factor is $\alpha = 1.0\times10^3$.

Figures 5–7 show the analytical and numerical solutions obtained by the three meshless methods at $x_1 = 1/6$. We choose $d_{\max}$ to be 1.7 for the CVRKPM, 1.9 for the EFG method, and 2.7 for the RKPM. Then, the CVRKPM and EFG method have greater computational accuracy.

As regards the computational speeds of the three methods, under the same accuracy, the CVRKPM is faster than the other two methods. As shown in Fig. 8, under the same accuracy, the CVRKPM requires 144 nodes and CPU time of 211 s, the EFGM requires 144 nodes and CPU time of 361 s, and the RKPM requires 225 nodes and CPU time of 267 s. Then, the CVRKPM has higher computational efficiency.

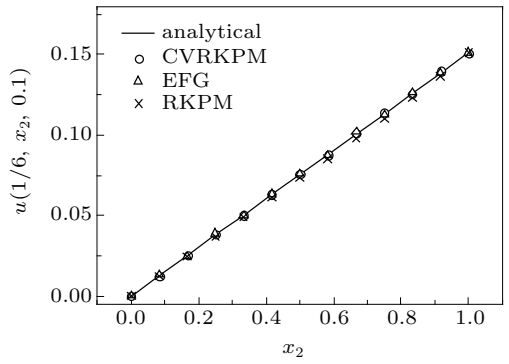


Fig. 5. Comparison of the solutions of CVRKPM, RKPM, and EFG method with the analytical one at $x_1 = 1/6$ at time $t = 0.1$ s.

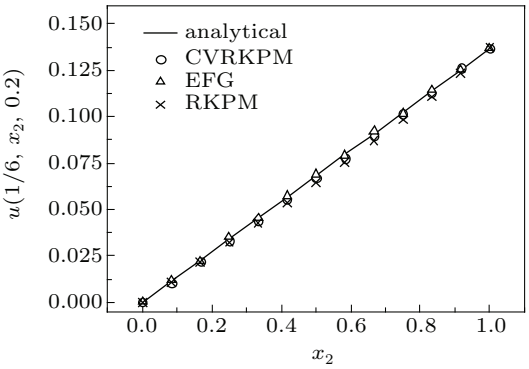


Fig. 6. Comparison of the solutions of CVRKPM, RKPM, and EFG method with the analytical one at $x_1 = 1/6$ at time $t = 0.2$ s.

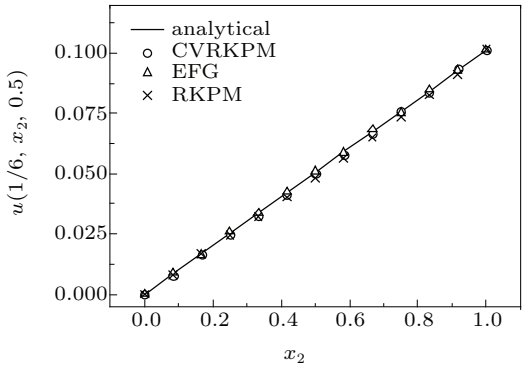


Fig. 7. Comparison of the solutions of CVRKPM, RKPM, and EFG method with the analytical one at $x_1 = 1/6$ at time $t = 0.5$ s.

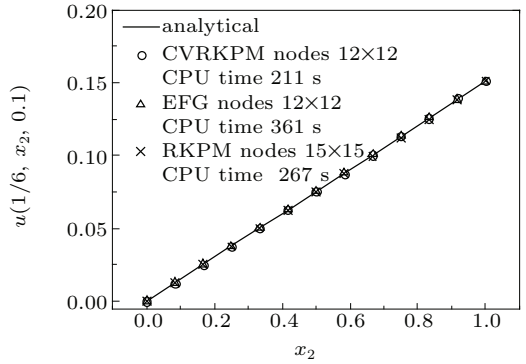


Fig. 8. Comparison between CPU time for a given accuracy at $x_1 = 1/6$ at time $t = 0.1$ s.

5. Conclusions

Based on the ICVMLS approximation, we present the CVRKPM for 2D advection–diffusion problems. An example of diffusion-dominated advection–diffusion equation and an example of advection dominated advection- diffusion equation are used to study the newly developed meshless method. We can draw the following conclusions. (i) The CVPKRM has much better accuracy and efficiency than the RKPM, and it also has better computational efficiency than the EFG method. (ii) To reduce the error of solution obtained by the CVRKPM, nodes can be increased, but it also increases the computation time. (iii) The solutions of the CVRKPM are in excellent agreement with the analytical solutions of both the diffusion-dominated advection–diffusion equations and advection-dominated ones. In a word, the CVRKPM has good potential in solving problems in engineering and science which are governed by various types of partial differential equations.

References

[1] Knopp T, Lube G and Rapin G 2002 *Comput. Meth. Appl. Mech. Eng.* **191** 2997
[2] Franca L P, Hauke G and Masud A 2006 *Comput. Meth. Appl. Mech. Eng.* **195** 1560
[3] John V and Knobloch P 2007 *Comput. Meth. Appl. Mech. Eng.* **196** 2197
[4] Turner D Z, Nakshatrala K B and Hjelmstad K D 2011 *Int. J. Number. Meth. Fl.* **66** 64
[5] John V and Novo J 2012 *J. Comp. Phys.* **231** 1570
[6] Boztosun I and Charafi A 2002 *Eng. Anal. Boundary Element* **26** 889
[7] Ikeuchi M and Onishi K 1983 *App. Math. Model* **7** 115
[8] Noye B J and Tan H H 1989 *Int. J. Number. Meth. Fl.* **9** 75
[9] Belytschko T, Krongauz Y, Organ D, Fleming M and Krysl P 1996 *Comput. Meth. Appl. Mech. Eng.* **139** 3
[10] Zerroukat M, Power H and Chen C S 1998 *Int. Number. Meth. Eng.* **42** 1263
[11] Zhan Z, Liew K M, Chen Y M and Lee Y Y 2008 *Eng. Anal. Boundary Elements* **32** 241
[12] Zhang Z, Liew K M and Cheng Y M 2008 *Eng. Anal. Boundary Elements* **32** 241
[13] Cheng R J and Ge H X 2009 *Chin. Phys. B* **18** 4059
[14] Wang J F, Sun F X and Cheng Y M 2012 *Chin. Phys. B* **21** 090204
[15] Ren H P and Cheng Y M 2012 *Int. J. Comput. Mater. Sci. Eng.* **1** 1250011
[16] Zhang Z, Li D M, Chen Y M and Liew K M 2012 *Acta Mech. Sin.* **28** 808
[17] Cheng R J and Ge H X 2012 *Chin. Phys. B* **21** 040203
[18] Qin Y X and Cheng Y M 2006 *Acta Phys. Sin.* **55** 3215 (in Chinese)
[19] Qin Y X and Chen Y M 2008 *Chin. J. Mech. Eng.* **44** 95 (in Chinese)
[20] Li Z H, Qin Y X and Cui X C 2012 *Acta Phys. Sin.* **61** 080205 (in Chinese)
[21] Cheng Y M and Li J H 2005 *Acta Phys. Sin.* **54** 4463 (in Chinese)
[22] Chen Y M, Peng M J and Li J H 2005 *Acta Mech. Sin.* **37** 719 (in Chinese)
[23] Peng M J, Liu P and Chen Y M 2009 *Int. J. App. Mech* **1** 367
[24] Liu P, Peng J and Cheng Y M 2009 *Compu. Aided Eng.* **18** 11 (in Chinese)
[25] Liew K M and Chen Y M 2009 *Comput. Met. Appl. Mech Eng.* **198** 3925
[26] Peng M J, Li D M and Chen Y M 2011 *Eng. Struct.* **33** 127
[27] Cheng Y M, Wang J F and Bai F N 2012 *Chin. Phys. B* **21** 090203
[28] Cheng Y M, Li R X and Peng M J 2012 *Chin. Phys. B* **21** 090205
[29] Cheng Y M, Wang J F and Li R X 2012 *Int. J. Appl. Mech.* **4** 1250042
[30] Yang X L, Dai and Li Z F 2012 *Acta Phys. Sin.* **61** 050204 (in Chinese)
[31] Chen L and Cheng Y M 2008 *Acta Phys. Sin.* **5** 6047 (in Chinese)
[32] Chen L and Cheng Y M 2010 *Sci. China Phys Mech. Astron* **53** 954
[33] Chen L and Cheng Y M 2010 *Chin. Phys. B* **19** 090204
[34] Chen L, Liew K M and Cheng Y M 2010 *Interaction and Multiscale Mechanics: An International Journal* 27